

PAPER

Propofol regulates miR-1-3p/IGF1 axis to inhibit the proliferation and accelerates apoptosis of colorectal cancer cells

Ling-Ling Ye, Zhong-Gui Cheng, Xiao-E Cheng and Yuan-Lu Huang*

Department of Anesthesiology, The First Affiliated Hospital of Nanchang University, Nanchang 330006, China

*Correspondence address. Department of Anesthesiology, The First Affiliated Hospital of Nanchang University, No. 17, Yongwai Zheng Street, Nanchang 330006, Jiangxi, China. Tel: +86-18779865670; E-mail: 627327492@qq.com

Abstract

This study aimed to clarify the mechanism of propofol on proliferation and apoptosis of colorectal cancer (CRC) cell. SW620 and HCT15 cells were exposed to different concentrations of propofol, the proliferation and apoptotic rate, were measured by MTT, colony formation and flow cytometry assays, respectively. The expressions of miR-1-3p and insulin-like growth factors 1 (IGF1) were examined by real-time polymerase chain reaction (RT-qPCR). Western blot was employed to quantify the protein levels of IGF1 and apoptotic proteins. The molecular interaction between miR-1-3p and IGF1 was validated using dual-luciferase reporter assay. A xenograft tumor model was established to further assess the effects of propofol on CRC *in vivo*. Propofol dramatically decreased the proliferation and elevated apoptotic rate of CRC cells. RT-qPCR assay demonstrated that miR-1-3p was downregulated in CRC cells, and could be strikingly increased by propofol. Importantly, miR-1-3p inhibited IGF-1 expression through interacting with its 3'-UTR region, thus inactivating AKT/mTOR signals. Gain or loss of functional study revealed that miR-1-3p downregulation remarkably diminished the anti-tumor roles of propofol by directly inhibiting IGF1. *In vivo* study showed that propofol inhibited tumor growth by regulating miR-1-3p/IGF1 axis. Our data eventually elucidated that propofol suppressed CRC progression by promoting miR-1-3p which targeted IGF1. These results might provide a scientific basis for the application of propofol on the clinical surgery and the prognosis of patients with CRC.

Key words: AKT/mTOR signaling, colorectal cancer, insulin-like growth factor 1, miR-1-3p, propofol

Introduction

Colorectal cancer (CRC) is one of the most common and fatal malignant cancers worldwide, causing ~1.4 million diagnosed cases and 700 000 deaths every year [1]. Due to the high invasiveness, transitivity and poor prognosis, the incidence of CRC is still increasing year by year. In current, surgical resection is the principal strategy to treat CRC for the different clinical history, pathological features and involved molecular mechanisms [2]. It has reported that anesthesia can cause metabolic, inflammatory and immune changes during the perioperative period and affect

the long-term prognosis of patients after surgery, especially the recurrence of cancer [2, 3]. However, the underlying mechanism remains unclear.

Propofol (2, 6-diisopropylphenol) was extensively used for surgery and widely proved to be beneficial to cancer patients for its sedative, hypnotic and anti-tumor effects. For instance, propofol inhibited the HIF-1 α activity to prevent the aggressive phenotypes of cancer and worsened clinical outcome [4, 5]. Additionally, it was also reported that propofol could suppress the tumor growth by enhancing the cytotoxic T-lymphocytes

Received: 17 September 2020; Revised: 6 April 2021; Accepted: 29 April 2021

© The Author(s) 2021. Published by Oxford University Press. All rights reserved. For Permissions, please email: journals.permissions@oup.com

activity and reduce the immune cell functions to achieve the tumor evasion of host immune surveillance [6, 7]. Consistently, in terms of CRC, propofol was reported to inhibit cell proliferation, metastasis and epithelial-mesenchymal transition of CRC by regulating miR-124-3p/1/AKT3 axis [8, 9]. Besides, Wu et al. [10] identified that propofol anesthesia applied for CRC surgery was correlated to better survival rate of patients which in irrespective of tumor-node-metastasis stage, compared with Desflurane. As the widespread application of propofol, more investigations about the underlying mechanisms of propofol need to be studied.

miRNAs, as small noncoding transcripts, play a vital regulation in cell proliferation, apoptosis, oxidative stress, inflammatory responses and so on. The abnormal expressed miRNAs were considered as one of contributors in the onset and development of cancers. miR-1-3p, belonging to the miR1/miR133 cluster, was reported to be general downregulated and suppressed the proliferation and invasion of tumor cells in lung cancer (Jiao et al., 2018), oral squamous cell carcinoma [11], prostate cancer [12] and hepatocellular carcinoma [13]. Previous evidences have identified that the expression of miR-1-3p was downregulated in CRC [14, 15]. Interestingly, miR-1-3p was discovered to be highly expressed in circulating vesicles of CRC patients who treated propofol [16], whereas its underlying correlation remain not been elucidated.

In the present study, the effects of propofol on the cell proliferation and apoptosis of CRC were evaluated in SW620 and HCT15 cell lines. To further elaborate the action of mechanism of propofol, we measured the expressive and functional correlation between propofol and miR-1-3p/IGF1 axis. Our finding aimed to provide a theoretical basis for the application of propofol on the clinical surgery and prognosis of patients with CRC.

Materials and Methods

Cell culture and drug treatment

The human CRC cell lines (SW620 and HCT15) and normal epithelial colon cell line (NCM460) were obtained from American Type Culture Collection (ATCC, Manassas, VA, USA). SW620 was grown in Dulbecco's modified eagle medium, and HCT15 and NCM460 cells were maintained in RPMI 1640 medium (Invitrogen, Carlsbad, CA, USA). All mediums used in this work were mixed with 10% fetal bovine serum (Gibco, Carlsbad, CA, USA), 100-U/ml penicillin (Gibco) and 100-mg/ml streptomycin (Gibco). Cells were cultured in 5% CO₂/95% humidified air at 37°C.

Propofol was obtained from Sigma-Aldrich (St Louis, MO, USA) and diluted in dimethyl sulfoxide (DMSO) (Sigma-Aldrich). Then, a series of concentrations (0, 5, 10 and 20 µg/ml) of propofol in medium were prepared as previous described [17].

MTT assay

Cells were seeded in 96-well plate with a density of 2000 cells/well. After treatment or transfection for 24 h, 20-µl 3-(4,5-dimethyl thiazol-2-yl)-5-diphenyl tetrazolium bromide (MTT) solutions (5 mg/ml, Sigma, MO, USA) were added in each well for incubation 4 h at 37°C. After removing MTT solution, 150-µl DMSO was added and then shaken for 5 min. The absorbance of each well was measured at 490 nm using a microplate reader (Tecan, Mannedorf, Switzerland).

Colony formation assay

For the colony formation assay, cells were plated in 6-wells plates at a density of 300 cells/well and cultured in complete medium with or without propofol (20 µg/ml). After 48 h, the medium was replaced with fresh drug-free medium and further incubated for 8 days in order to form cell clones. Next, cells were fixed and stained with Coomassie blue. Colonies consisting more than 50 cells were counted. Pictures were then taken using a digital camera to record the results.

Flow cytometric detection

The cell apoptosis assay was performed using propidium iodide (PI) and Annexin V-FITC double-staining (KeyGEN, Nanjing, China). Cells were plated in 6-wells plates at a density of 1×10^5 cells per well. After treatment or transfection for 48 h, the cells were collected and washed three times with ice-cold PBS, then centrifuged at 1500 rpm for 5 min. Cells were re-suspended by 500-ml binding buffer containing 5-µl Annexin V-FITC and 5-µl PI, and then incubated for 30 min in dark condition. Subsequently, the cells were analyzed using Fluorescence activated Cell Sorting (BD Biosciences, USA).

Cell transfection

miR-1-3p mimics and inhibitor, the overexpression plasmids of IGF1 (pcDNA-IGF1) and small interfering RNA (siRNA) targeting IGF1 as well as their corresponding controls (mimics NC, inhibitor NC, pcDNA-NC, si-NC) were all designed and synthesized by Genepharma (Shanghai, China). Cell transfection was carried out by using Lipofectamine 2000 (Invitrogen, USA). The transfection efficiencies were measured by RT-qPCR after transfection for 48 h.

RNA extraction and RT-qPCR analysis

Total RNA was isolated using Trizol® (Invitrogen, USA) according to the manufacturer's protocol. cDNA was synthesized using SuperScript First-Strand Synthesis kit (Invitrogen, USA). Real-time qPCR was performed using SYBR Permex Ex Taq (Takara, Dalian, China) in 7500 Real-time PCR System (Applied Biosystems, USA) to determine the expressions of miR-1-3p and IGF1. GAPDH and U6 were used to normalize IGF1 and miR-1-3p expression, respectively. Data were quantified using $2^{-\Delta\Delta Ct}$ method. The primers in this work are presented as Table 1.

Protein extraction and western blot assay

Cells were lysed in RIPA buffer (Sigma-Aldrich, St. Louis, MO, USA) to extract total proteins. The concentrations of total proteins were quantified using BCA protein assay kit (Sigma-Aldrich). Then, equal amount proteins were separated by 10% sodium dodecyl sulfate-polyacrylamide gel electrophoresis and transferred onto polyvinylidene fluoride membrane (PVDF). The membranes were cut off the corresponding region of the whole membrane according to the molecular weight of the proteins after Ponceau red staining. After blocking with 5% nonfat milk dissolved in TBS buffer for 1 h, the membranes were incubated with different primary antibodies including Anti-IGF1 (1:1000, Abcam, Cambridge, UK), anti-Bcl-2 (1:1000, Abcam), cleaved-caspase3 (1:500, Abcam), anti-cleaved-caspase

9 (1:200, Abcam), anti-p-AKT (1:200, Abcam), anti-p-mTOR (1:900, Abcam), anti-AKT (1:500, Abcam) and anti-mTOR (1:2000, Abcam) for overnight at 4°C. Then, the membranes were incubated with HRP-conjugated secondary antibody (1:5000, Abcam) for 2 h at room temperature. After that, the images were performed using the enhanced chemiluminescence (Sigma-Aldrich). The bands were calculated by Image J software.

Dual-luciferase reporter gene assay

The wild-type IGF-1 (wt-IGF-1) and mutant IGF-1 (mut-IGF-1) with/without the putative binding site of miR-1-3p were constructed into the pGL3-control luciferase reporter vectors (Promega, Madison, WI, USA) and transfected into SW620 cells, respectively. Then, cells containing wt-IGF-1 or mut-IGF-1 vectors were co-transfected with miR-1-3p mimics or mimics NC. The Luciferase activity was measured 48 h post-transfection. Renilla luciferase acted as internal control.

Construction of CRC xenograft mice model

Twenty male nude mice (6 weeks, 20 ± 2 g) were purchased from SJA Laboratory Animal Company (Hunan, China). All mice were housed at $25 \pm 1^\circ\text{C}$ under 12-h light/12-h dark cycle with a relative humidity of 30–60%, a standard pellet diet with water ad libitum. All mice were randomly divided into four groups, then different treated SW620 cells (5×10^6 cells) were transplanted into left axillary subcutaneous: model group (untreated SW620 cells), model + DMSO group (SW620 cells was treated by DMSO for 24 h), model + propofol (SW620 cells was treated by 20- $\mu\text{g}/\text{ml}$ propofol for 24 h) and model + propofol + miR-1-3p inhibitor (SW620 cells were transfected miR-1-3p inhibitor and exposed to 20- $\mu\text{g}/\text{ml}$ propofol for 24 h). The tumor volume was measured every 5 days for 1 month. On the 30th days, mice were euthanized by carbon dioxide; the tumor tissues were dissected, cleaned for further assays. All animal experiments were approved by The First Affiliated Hospital of Nanchang University.

Statistical analysis

All experiments were conducted in triplicate, and data were expressed as the means \pm standard deviations. The data were analyzed using one-way ANOVA, followed by the Least Significant Difference *post hoc* test. A *P*-value <0.05 was considered statistically significant.

Results

Effects of propofol on proliferation and apoptosis of CRC cells

SW620 and HCT5 cells were exposed to a serious concentration of propofol (0, 5, 10 and 20 $\mu\text{g}/\text{ml}$) for 24 h, and then, the cell viability was evaluated. As shown in Fig. 1A, propofol treatment suppressed the viability of tumor cells at a dose-dependent manner. Therefore, 20- $\mu\text{g}/\text{ml}$ propofol was used in the followed experiments. Consistently, the result of clone formation assay also described that the number of clones was markedly reduced by propofol treatment compared with control group (Fig. 1B), indicating that propofol served an anti-proliferative role in CRC cells. Compared with control group, propofol treatment significantly enhanced the apoptotic rates of tumor cells and the pro-apoptotic proteins (cleaved-caspase 3 and cleaved-caspase

Table 1: primers used for qPCR analysis

Gene	Primer sequences
miR-1-3p forward	5'-TGGAATGTAAAGAAGTATGTAT-3'
miR-1-3p reverse	5'-CCTGAACCCACTTCTGCTTG-3'
IGF-1 forward	5'-ACCCGGACTACTTCCAGCGCT-3'
IGF-1 reverse	5'-CACAGAAGCTTCGTTGAGAA-3'
STC2 forward	5'-TCTTGTGAGATTCCGGGCTT-3'
STC2 reverse	5'-ACAGGTCGTGCTTGAGGTAG-3'
FN1 forward	5'-CGGTGGCTGTGAGTCAAAG-3'
FN1 reverse	5'-AAACCTCGGCTTCCTCCATAA-3'
BDNF forward	5'-CATCCAGTTCACCAGGT-3'
BDNF reverse	5'-CCATGGTCCGCACAGCT-3'
E2F5 forward	5'-TCTTACACAGCTTGCATCGCGGG-3'
E2F5: reverse	5'-GCGCGATGCAAGCTGTGTAAGAGG-3'
U6 forward	5'-CTCGCTTCGGCAGCACA-3'
U6 reverse	5'-AACGCTTCACGAATTTGCGT-3'
GAPDH forward	5'-AGGTCGGTGTGAACGGATTTG-3'
GAPDH reverse	5'-GGGTCGTTGATGGCAACA-3'

9) levels, while decreased the anti-apoptotic protein (Bcl-2) level (Fig. 1C and D). That all, these finding disclosed that propofol play an anti-tumor effect in CRC cells progression.

miR-1-3p was modulated by propofol and participated in propofol mediated anti-tumor effects

Here, we firstly detected the expression of miR-1-3p in CRC cell lines by RT-qPCR assay. Compared with NCM460 cells, miR-1-3p expression showed a great decrease in SW620 and HCT15 cells (Fig. 2A). Interestingly, after propofol treatment, the expression level of miR-1-3p was significantly elevated (Fig. 2B). Therefore, we further evaluated the effects of miR-1-3p on propofol-mediated anti-tumor roles. Figure 2C described that the promoting effect of propofol on miR-1-3p expression was dramatically eliminated by transfecting with miR-1-3p inhibitor. Cell proliferative detection presented that miR-1-3p knockdown significantly reversed the inhibitory effects of propofol on cell viability and clone formation (Fig. 2D and E). Similarly, the increased apoptotic rate, protein levels of cleaved-caspase 3 and cleaved-caspase 9, and the decrease of Bcl2 level mediated by propofol were significantly weakened after miR-1-3p inhibitor treatment (Fig. 2F and G). Thus, it is concluded that miR-1-3p was participated in the regulation of propofol on proliferation and apoptosis of CRC cells, indicating that miR-1-3p is the target of propofol on CRC cells.

miR-1-3p suppressed the activation of AKT/mTOR signaling by targeted regulating IGF-1

To further analyze the molecular mechanism of miR-1-3p in CRC, we selected few possible downstream oncogenic targets of miR-1-3p. The binding sites and properties of miR-1-3p with IGF1, STC2, FN1, BDNF or E2F5 were predicted by TargetScan software (Fig. S1A). qRT-PCR assay showed that the mRNA levels of IGF1, STC2, FN1, BDNF and E2F5 were all inhibited by miR-1-3p overexpression and increased by miR-1-3p inhibition, especially IGF1 (Fig. S1B). Subsequently, the mutant-/wild-binding site between miR-1-3p and IGF1 was displayed in Fig. 3A. The targeted relationship between miR-1-3p and IGF1 was also validated by dual luciferase reporter assay. As shown

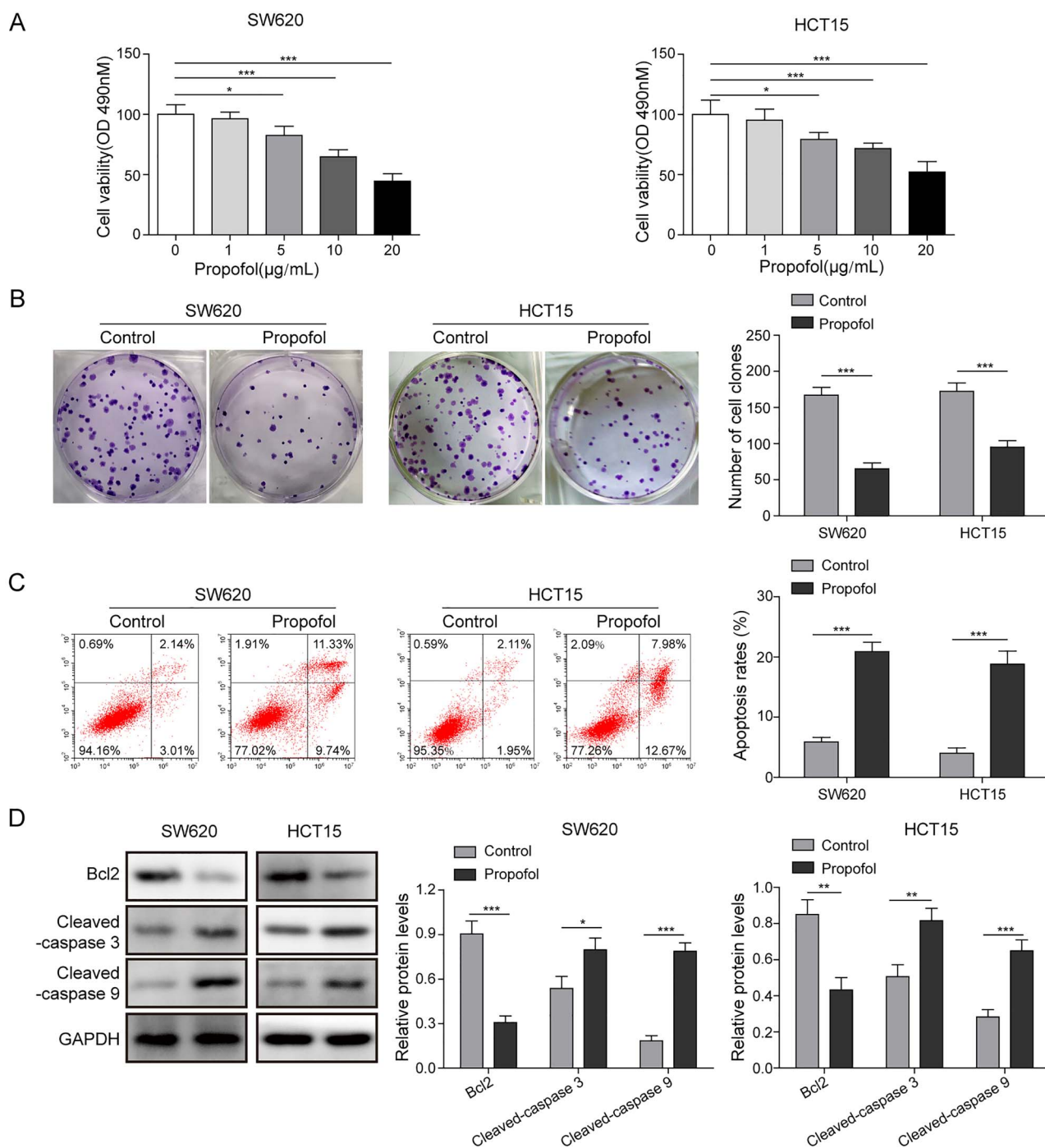


Figure 1: Effects of propofol on proliferation and apoptosis of CRC cells. SW620 and HCT15 cells were exposed in a serious concentration of propofol (0, 1, 5, 10 and 20 µg/ml) for 24 h. Then, the cell proliferation was detected by MTT assay (A) and colony formation assay (B). SW620 and HCT15 cells were exposed in 20-µg/ml propofol for 24 h. (C) Cell apoptotic rate was determined by flow cytometry assay. (D) The apoptotic protein levels were quantified by western blotting. * $P < 0.05$, ** $P < 0.01$ and *** $P < 0.001$.

in Fig 3B, the relative luciferase activity was decreased by miR-1-3p mimics in SW620 cells co-transfected with wt-IGF-1 vectors, whereas no significant difference was observed in SW620 cells containing mut-IGF-1 vectors. Furthermore, miR-1-3p overexpression by transfection miR-1-3p mimics markedly inhibited IGF1 expression, while miR-1-3p inhibition by transfection miR-1-3p inhibitor obviously enhanced IGF1 expression (Fig. 3C). AKT/mTOR signaling was an important

carcinogenic signaling pathway. As shown in Fig 3D, the pcDNA-IGF1 vectors markedly enhanced the IGF1 expression in miR-1-3p overexpressing SW620 and HCT15 cells. Western blot assay revealed that miR-1-3p overexpression inhibited the protein level of IGF1 and phosphorylation of AKT and mTOR, whereas restoration of IGF1 significantly diminished these inhibitory effects mediated by miR-1-3p overexpression (Fig. 3E). Taken together, miR-1-3p negatively regulated IGF1 expression by

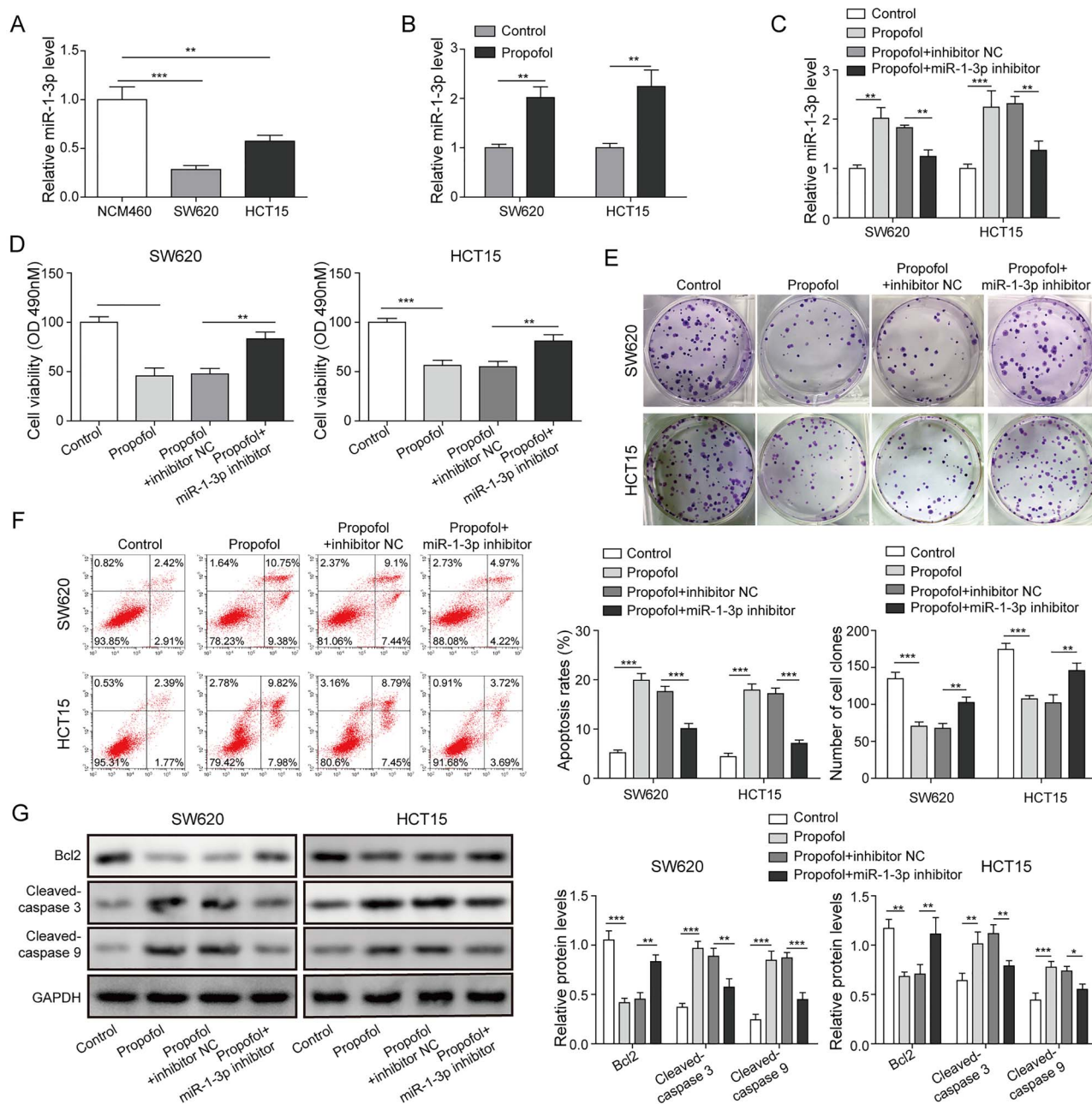


Figure 2: miR-1-3p was modulated by propofol and participated in the regulation of propofol mediated anti-tumor effects. (A) The expression of miR-1-3p in NCM460, SW620 and HCT15 cells was detected by RT-qPCR assay. (B) Effect of propofol on the expression of miR-1-3p was assessed by RT-qPCR assay. Inhibitor NC or miR-1-3p inhibitor was transfected into SW620 and HCT15 cells for 48 h, then exposed in 20- μ g/ml propofol condition for 24 h. (C) The expression of miR-1-3p was evaluated by RT-qPCR assay. (D) Cell viability was tested by MTT assay. (E) Cell proliferation was detected by clone formation assay. (F) Cell apoptotic rate was calculated by flow cytometry assay. (G) The levels of apoptotic proteins were quantified by western blotting. * $P < 0.05$, ** $P < 0.01$ and *** $P < 0.001$.

directly targeting its 3'-UTR, and thus inactivating AKT/mTOR1 signaling.

Knockdown of IGF-1 reversed the inhibitory effects of miR-1-3p downregulation on propofol-mediated anti-tumor roles

RT-qPCR result disclosed that propofol significantly downregulated IGF1 mRNA level, while it was reversed by silencing miR-1-3p (Fig. 4A). Next, si-IGF1 vectors were transfected into SW620

and HCT15 cells and prominently reduced IGF1 expression (Fig. 4B). Subsequently, cells were co-transfected with miR-1-3p inhibitor and exposed in medium containing propofol. Figure 4C demonstrated that knockdown of miR-1-3p abolished the inhibitory effects of propofol on the protein levels of IGF1 and AKT/mTOR signaling, while co-silencing IGF1 obviously restored the effects of propofol. Followed detection study on cell viability displayed that IGF1 silence significantly diminished the inhibitory effect of miR-1-3p downregulation on the anti-proliferation role of propofol (Fig. 4D). Similar trend was observed in the data of apoptotic detections. The protective effect of

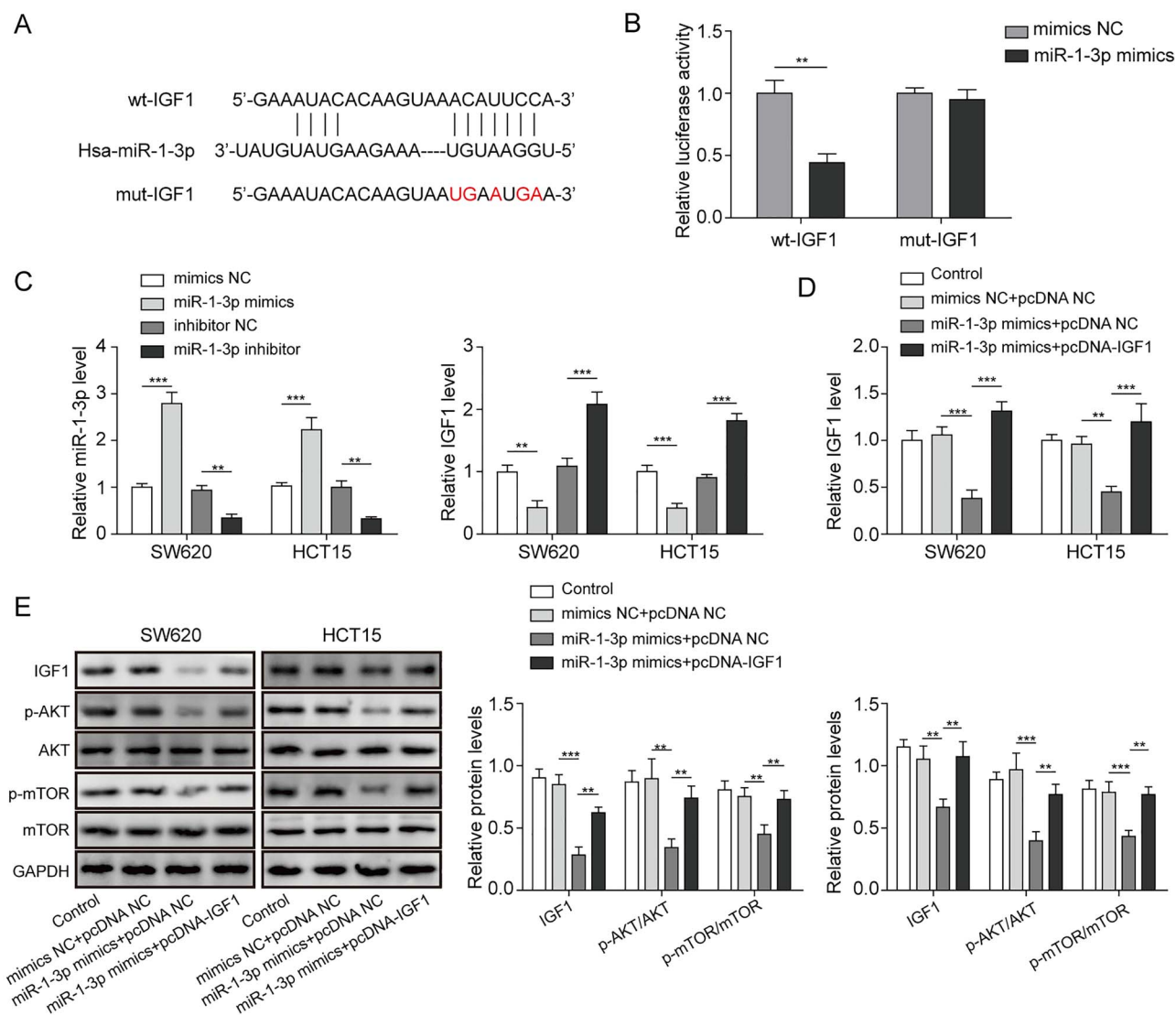


Figure 3: miR-1-3p suppressed the activation of AKT/mTOR signaling by targeted regulating IGF-1. (A) The bioinformatics analysis was used to predict the binding site between miR-1-3p and IGF1. (B) The molecular interaction between miR-1-3p and IGF-1 was validated by dual luciferase reporter assay. (C) SW620 and HCT15 cells were transfected with miR-1-3p mimics or inhibitor for 48 h; the expression levels of miR-1-3p and IGF-1 after transfection were quantified by RT-qPCR assay. (D) SW620 and HCT15 cells were transfected with miR-1-3p mimics or co-transfected with miR-1-3p and pcDNA3.1-IGF1 for 48 h; the expression level of IGF1 was quantified by RT-qPCR assay. (E) The levels of IGF1 and AKT/mTOR-related proteins were quantified by western blotting. * $P < 0.05$, ** $P < 0.01$ and *** $P < 0.001$.

miR-1-3p knockdown on propofol stimulated cell apoptosis was reversed by IGF1 downregulation (Fig. 4E). Likewise, IGF1 downregulation also abolished the regulatory impacts of miR-1-3p knockdown on apoptotic proteins levels (Fig. 4F), which recovered the pro-apoptotic effects of propofol. These results inferred that miR-1-3p/IGF1 axis was a downstream functional signaling of propofol in CRC progression.

Propofol inhibited tumor growth by facilitating miR-1-3p *in vivo*

The effects of propofol on CRC were also measured *in vivo*. As shown in Fig. 5A, compared with Model and Model + DMSO groups, the tumor volume was decreased after propofol treatment, while this effect was reversed by miR-1-3p inhibition. Similarly, the tumor size and weight were also significantly inhibited by propofol, and these inhibitory effects were decreased

by miR-1-3p inhibitor co-treatment (Fig. 5B and C). qRT-PCR assay showed that compared with Model group, miR-1-3p was upregulated in propofol group and further decreased in Model+Propofol+miR-1-3p inhibitor group (Fig. 5D). Moreover, we also found that the protein levels of IGF1 and Bcl2 were significantly decreased, while cleaved-caspase 3 and cleaved-caspase 9 were obviously increased after propofol treatment, whereas co-treatment of miR-1-3p inhibitor markedly diminished the effects of propofol (Fig. 5E). These data confirmed that propofol suppressed tumor growth by modulating miR-1-3p/IGF1 axis.

Discussion

CRC is the third most deadly cancer worldwide and the top five of high mortality cancers in China [18, 19]. Surgical resection-based chemotherapies are widely used in clinic as the most effective and mainstay treatment options [20]. However, the recurrent rate

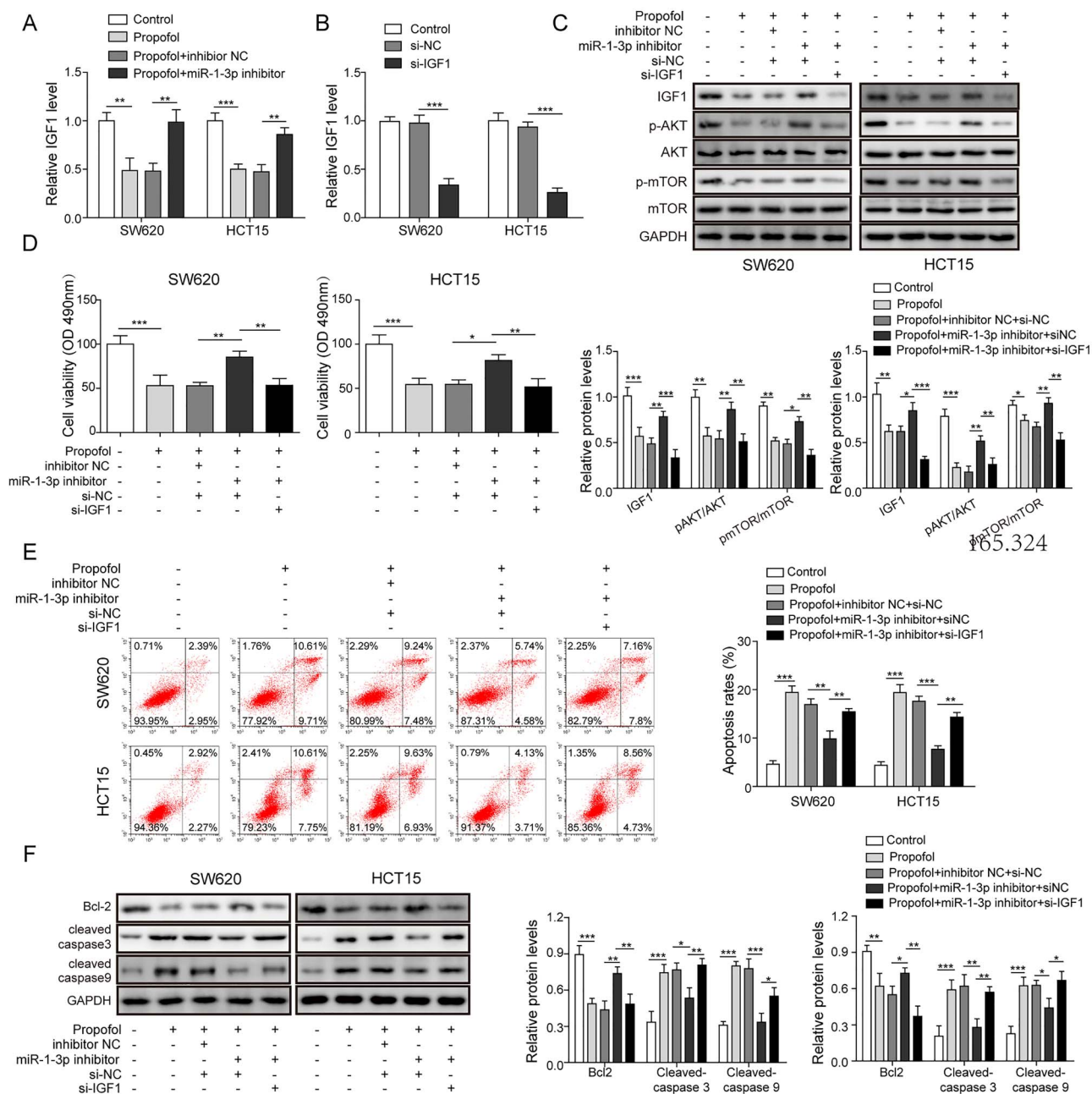


Figure 4: Knockdown of IGF-1 reversed the inhibitory effects mediated by miR-1-3p downregulation on the anti-tumor roles of propofol. (A) SW620 and HCT15 cells were transfected with miR-1-3p inhibitor, then exposed in 20- μ g/ml propofol for 24 h; the expression of IGF1 was calculated by RT-qPCR assay. (B) SW620 and HCT15 cells were transfected with si-IGF1 or si-NC; the expression of IGF1 was detected by RT-qPCR assay. SW620 and HCT15 cells were transfected with miR-1-3p inhibitor or co-transfected with miR-1-3p inhibitor and si-IGF1, then cells were stimulated in 20- μ g/ml propofol for 24 h; then, (C) the levels of IGF1 and AKT/mTOR signaling-related proteins were detected by western blotting. (D) Cell viability was tested by MTT assay. (E) Cell apoptotic rate was determined by flow cytometry. (F) The levels of apoptotic proteins were evaluated by western blotting. * $P < 0.05$, ** $P < 0.01$ and *** $P < 0.001$.

of CRC at first five years after surgery is 20–30% [21]. Therefore, it is important to clarify the underlying factors that affect the long-term prognosis of patients during the perioperative period. Anesthesia, as an unavoidable factor during surgery, attracted more and more attentions. It is reported that anesthesia and the anesthesia technique could affect the outcomes of cancer patients [3, 22]. In our study, we investigated that the biological influence and specific molecular mechanism of propofol in CRC further confirming the therapeutic value in clinical CRC surgery.

Propofol was a widely used anesthesia in CRC resection surgery due to some non-anesthetic effects including anti-inflammatory, anti-oxidant, neuroprotective and so on [23]. Recently, a great number of reports have proved the anti-tumor effects of propofol in several cancers. For instance, Zhang *et al.* [17] confirmed that propofol suppressed the capabilities of proliferation, migration and invasion of gastric cancer by promoting miR-195. Ren *et al.* [24] also revealed that propofol inhibited CRC tumorigenesis through repressing lncRNA HOXA11-AS/let-7/ABCC10 ceRNA network. Additionally, a large number of studies

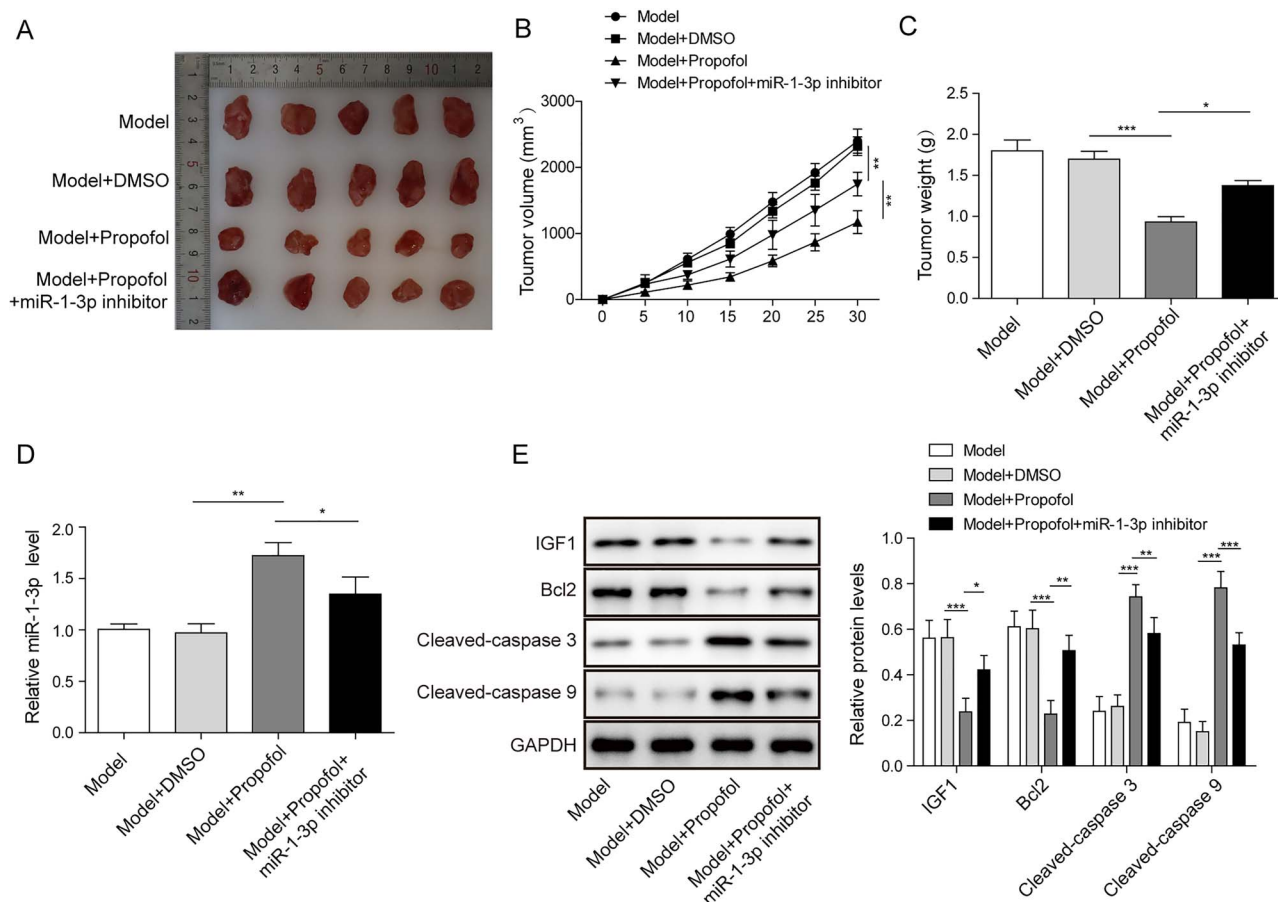


Figure 5: Effect of propofol on tumor growth of CRC *in vivo*; 20 male nude mice were randomly divided into four groups (model group, model + DMSO group, model + propofol and model + propofol + miR-1-3p inhibitor) to establish mouse xenograft model. (A) Photographs of transplanted tumor in nude mice. (B) Changes of tumor size. (C) Changes of tumor weight. (D) The expression level of miR-1-3p was calculated by RT-qPCR assay. (E) The levels of IGF1 and apoptotic proteins were assessed by western blot. * $P < 0.05$, ** $P < 0.01$ and *** $P < 0.001$.

have shown that in nude mouse models, propofol inhibited the growth of xenograft tumors of a variety of cancers, such as cervical cancer, lung cancer and pancreatic cancer [25–27]. Consistently, we also demonstrated the anti-tumor roles of propofol, that is propofol significantly suppressed the tumor growth *in vivo*, and inhibited cell proliferation while promoted apoptosis of SW620 and HCT15 cells *in vitro*, further confirming the anti-tumor roles of propofol in CRC development.

A pilot study focused on the propofol and sevoflurane in circulating microRNAs profile of CRC patients showed that miR-1-3p was enriched in circulating vesicles of CRC patients who received propofol anesthesia for tumor resection [16]. Moreover, a variety of miRNAs were reported to correlate to the regulation of propofol in cancer development, such as miR-124-3p.1 and miR-195 [8, 17]. Hence, we further studied the potential association between propofol and miR-1-3p. The data displayed that miR-1-3p could be upregulated by propofol, which was consisted with previous reports. In CRC, miR-1-3p has a tumor suppressive effect in most existing studies. For example, miR-1-3p was remarkably downregulated in stage II/III CRC tissues and served as a diagnostic biomarker [15]. miR-1-3p was also reported to inhibit tumorigenesis and migration by regulating NOTCH3 [28]. In present study, our data illustrated that miR-1-3p was down-regulated in SW620 and HCT15 cells compared with NCM

460. Importantly, miR-1-3p downregulation reversed the anti-proliferative and pro-apoptotic effects of propofol in CRC cells. Therefore, miR-1-3p was considered as a target of propofol in CRC progression.

IGF-1, as an anti-apoptotic factor that regulates the proliferation and survival of various cell types, was identified as a predictive marker or a new molecular therapeutic approach of CRC [29]. IGF1 is up-regulated in CRC and could promote the invasion of CRC cells and induce apoptosis [29]. In this context, we have validated a directly binding relationship between IGF1 and miR-1-3p in SW620 cells, indicating that IGF1 was a target of miR-1-3p, which also supported by Hua *et al.* and Liu *et al.* reports [30, 31]. Besides, Zhang *et al.* revealed that IGF1 could interact with IGF1R and activated AKT/mTOR signaling, eventually affecting cell proliferation, apoptosis and metastasis [32–34]. Here, miR-1-3p was verified to suppress the activation of AKT/mTOR signaling by targeted regulating IGF-1. Furthermore, our data also identified that propofol inhibited the activation of AKT/mTOR signaling by regulating miR-1-3p/IGF1 axis. Rescue experiments discovered that miR-1-3p downregulation mediated inhibitory impacts on the anti-tumor effects of propofol were eliminated by IGF1 silence, implying that propofol may inhibit proliferation and promoted cell apoptosis by regulating miR-1-3p-mediated IGF1/AKT/mTOR signal pathway.

Conclusion

In conclusion, our data elucidated that propofol served anti-tumor effects in CRC progression by regulating miR-1-3p/IGF-1 axis. These results might provide a scientific basis for the use of propofol on the clinical surgery and the prognosis of patients with CRC.

Acknowledgements

Not applicable.

Funding

None.

Conflicts of interest statement

The authors declare that they have no conflict of interest.

Abbreviations

CRC, colorectal cancer; DMSO, dimethyl sulfoxide; IGF-1, insulin-like growth factor 1; LSD, least significant difference; mTOR, mammalian target of rapamycin; MTT, 3-(4,5-dimethyl thiazol-2-yl)-5-diphenyl tetrazolium bromide; NC, negative control; SD, standard deviations; RT-qPCR, real-time polymerase chain reaction; NCM460, normal epithelial colon cell line; ATCC, American Type Culture Collection; DMEM, Dulbecco's modified eagle medium; FBS, fetal bovine serum; DMSO, dimethyl sulfoxide; PI, propidium iodide, siRNA, small interfering RNA, SDS-PAGE; sulfate-polyacrylamide gel electrophoresis, PVDF; polyvinylidene fluoride membrane

References

- Moreno EC, Pascual A, Prieto-Cuadra D et al. Novel molecular characterization of colorectal primary tumors based on miRNAs. *Cancers (Basel)* 2019;**11**:346.
- Novak-Jankovic V, Markovic-Bozic J. Regional anaesthesia in thoracic and abdominal surgery. *Acta Clin Croat* 2019;**58**:96–100.
- Kurosawa S, Kato M. Anesthetics, immune cells, and immune responses. *J Anesth* 2008;**22**:263–77.
- Takabuchi S, Hirota K, Nishi K et al. The intravenous anesthetic propofol inhibits hypoxia-inducible factor 1 activity in an oxygen tension-dependent manner. *FEBS Lett* 2004;**577**:434–8.
- Tavare AN, Perry NJS, Benzonana LL et al. Cancer recurrence after surgery: direct and indirect effects of anesthetic agents*. *Int J Cancer* 2012;**130**:1237–50.
- Inada T, Kubo K, Shingu K. Possible link between cyclooxygenase-inhibiting and antitumor properties of propofol. *J Anesth* 2011;**25**:569–75.
- Kushida A, Inada T, Shingu K. Enhancement of antitumor immunity after propofol treatment in mice. *Immunopharmacol Immunotoxicol* 2008;**29**:477–86.
- Li Y, Dong W, Yang H, Xiao G. Propofol suppresses proliferation and metastasis of colorectal cancer cells by regulating miR-124-3p.1/AKT3. *Biotechnol Lett* 2020;**42**:493–504.
- Xu K, Tao W, Su Z. Propofol prevents IL-13-induced epithelial-mesenchymal transition in human colorectal cancer cells. *Cell Biol Int* 2018;**42**:985–93.
- Wu ZF, Lee MS, Wong CS et al. Propofol-based total intravenous anesthesia is associated with better survival than desflurane anesthesia in colon cancer surgery. *Anesthesiology* 2018;**129**:932–41.
- Wang Z, Wang J, Chen Z et al. MicroRNA-1-3p inhibits the proliferation and migration of oral squamous cell carcinoma cells by targeting DKK1. *Biochem Cell Biol* 2018;**96**:355–64.
- Li SM, Wu HL, Yu X et al. The putative tumour suppressor miR-1-3p modulates prostate cancer cell aggressiveness by repressing E2F5 and PFTK1. *J Exp Clin Cancer Res* 2018;**37**:219.
- Zhang H, Zhang Z, Gao L et al. miR-1-3p suppresses proliferation of hepatocellular carcinoma through targeting SOX9. *Onco Targets Ther* 2019;**12**:2149–57.
- Wang JY, Huang JC, Chen G, Wei DM. Expression level and potential target pathways of miR-1-3p in colorectal carcinoma based on 645 cases from 9 microarray datasets. *Mol Med Rep* 2018;**17**:5013–20.
- Wu X, Li S, Xu X et al. The potential value of miR-1 and miR-374b as biomarkers for colorectal cancer. *Int J Clin Exp Pathol* 2015;**8**:2840–51.
- Buschmann D, Brandes F, Lindemann A et al. propofol and sevoflurane differentially impact MicroRNAs in circulating extracellular vesicles during colorectal cancer resection: a pilot study. *Anesthesiology* 2020;**132**:107–20.
- Zhang W, Wang Y, Zhu Z et al. Propofol inhibits proliferation, migration and invasion of gastric cancer cells by up-regulating microRNA-195. *Int J Biol Macromol* 2018;**120**:975–84.
- Cunningham D, Atkin W, Lenz HJ et al. Colorectal cancer. *Lancet* 2010;**375**:1030–47.
- Rawla P, Sunkara T, Barsouk A. Epidemiology of colorectal cancer: incidence, mortality, survival, and risk factors. *Prz Gastroenterol* 2019;**14**:89–103.
- Deng FL, Ouyang MW, Wang XF et al. Differential role of intravenous anesthetics in colorectal cancer progression: implications for clinical application. *Oncotarget* 2016;**7**:77087–95.
- Young PE, Womeldorph CM, Johnson EK et al. Early detection of colorectal cancer recurrence in patients undergoing surgery with curative intent: current status and challenges. *J Cancer* 2014;**5**:262–71.
- Snyder GL, Greenberg S. Effect of anaesthetic technique and other perioperative factors on cancer recurrence. *Br J Anaesth* 2010;**105**:106–15.
- Altenburg JD, Harvey KA, McCray S et al. A novel 2,6-diisopropylphenyl-docosahexaenoamide conjugate induces apoptosis in T cell acute lymphoblastic leukemia cell lines. *Biochem Biophys Res Commun* 2011;**411**:427–32.
- Ren YL, Zhang W. Propofol promotes apoptosis of colorectal cancer cells via alleviating the suppression of lncRNA HOXA11-AS on miRNA let-7i. *Biochem Cell Biol* 2020;**98**:90–8.
- Cui WY, Liu Y, Zhu YQ et al. Propofol induces endoplasmic reticulum (ER) stress and apoptosis in lung cancer cell H460. *Tumour Biol* 2014;**35**:5213–7.
- Gao Y, Yu X, Zhang F, Dai J. Propofol inhibits pancreatic cancer progress under hypoxia via ADAM8. *Journal of hepatobiliary-pancreatic sciences* 2019;**26**:219–26.
- Zhang D, Zhou XH, Zhang J et al. Propofol promotes cell apoptosis via inhibiting HOTAIR mediated mTOR pathway in cervical cancer. *Biochem Biophysical Res Commun* 2015;**468**:561–7.
- Furukawa S, Kawasaki Y, Miyamoto M et al. The miR-1-NOTCH3-Asef pathway is important for colorectal tumor cell migration. *PLoS One* 2013;**8**:e80609.

29. Peters G, Gongoll S, Langner C et al. IGF-1R, IGF-1 and IGF-2 expression as potential prognostic and predictive markers in colorectal-cancer. *Virchows Arch* 2003;**443**:139–45.
30. Hua Y, Zhang Y, Ren J. IGF-1 deficiency resists cardiac hypertrophy and myocardial contractile dysfunction: role of microRNA-1 and microRNA-133a. *J Cell Mol Med* 2012;**16**:83–95.
31. Liu K, Ying Z, Qi X et al. MicroRNA-1 regulates the proliferation of vascular smooth muscle cells by targeting insulin-like growth factor 1. *Int J Mol Med* 2015;**36**: 817–24.
32. Wang XW, Zhang YJ. Targeting mTOR network in colorectal cancer therapy. *World J Gastroenterol* 2014;**20**: 4178–88.
33. Zhang W, Feng G, Wang L et al. MeCP2 deficiency promotes cell reprogramming by stimulating IGF1/AKT/mTOR signaling and activating ribosomal protein-mediated cell cycle gene translation. *J Mol Cell Biol* 2018;**10**:515–26.
34. Zhou Y, Liang X, Chang H et al. Ampelopsin-induced autophagy protects breast cancer cells from apoptosis through Akt-mTOR pathway via endoplasmic reticulum stress. *Cancer Sci* 2014;**105**:1279–87.